Liquid Crystals
Publication details, including instructions for authors and subscription information:
http://www.informaworld.com/smpp/title~content=t713926090

Thermal properties and ionic conductivity of a polymer prepared by the *in situ* photopolymerization of a vinylimidazole monomer containing a mesogenic group

Hideyuki Yoshizawa[a]; Takashi Mihara[a]; Naoyuki Koide[a]
[a] Department of Chemistry, Faculty of Science, Science University of Tokyo, 1-3 Kagurazaka, Shinjuku-ku, Tokyo 162-8601, Japan

To cite this Article Yoshizawa, Hideyuki , Mihara, Takashi and Koide, Naoyuki(2005) 'Thermal properties and ionic conductivity of a polymer prepared by the *in situ* photopolymerization of a vinylimidazole monomer containing a mesogenic group', Liquid Crystals, 32: 1, 143 — 149

To link to this Article: DOI: 10.1080/02678290412331329152

URL: http://dx.doi.org/10.1080/02678290412331329152

Liquid Crystals, Vol. 32, No. 1, January 2005, 143–149

Thermal properties and ionic conductivity of a polymer prepared by the *in situ* photopolymerization of a vinylimidazole monomer containing a mesogenic group

HIDEYUKI YOSHIZAWA, TAKASHI MIHARA and NAOYUKI KOIDE*

Department of Chemistry, Faculty of Science, Science University of Tokyo, 1–3 Kagurazaka, Shinjuku-ku, Tokyo 162-8601, Japan

(*Received 7 June 2004; in final form 12 August 2004; accepted 26 September 2004*)

We have synthesized liquid crystalline polymers containing an imidazolium salt moiety and a mesogenic group by the *in situ* photopolymerization of a liquid crystalline vinylimidazole monomer in order to investigate the relationship between their thermal properties and ionic conductivity. A smectic phase was shown by the vinylimidazole monomer. The *in situ* photopolymerization of the monomer was carried out in the temperature range of the smectic phase. The polymer thus prepared displayed a highly ordered smectic phase in the temperature range between room temperature and about 200°C. The ionic conductivity of the polymer increased with increasing temperature. Anisotropic ionic conductivity behavior was observed for the polymer. The ionic conductivity of the polymer aligned homogeneously is larger than when homeotropically aligned.

Keywords: Imidazolium salt; Ionic conductivity; Liquid crystalline polymer; Photopolymerization

1. Introduction

Mixtures of poly(ethylene oxide) (PEO) and alkali metal salts have been studied intensively to determine the mechanism of the high ionic conductivity found [1]. The ionic conductivity of polymer electrolytes in the amorphous phase above the glass transition temperature has received much attention, because polymer chain motions in the amorphous phase create a dynamic, disordered environment which facilitates ion transport.

However, Gadjourova *et al*. reported that the ionic conductivity in the static and ordered environment of the crystalline phase of PEO was larger than that in the equivalent amorphous phase above the glass transition temperature [2]. This behavior implied that ionic conductivity may be favored in static and ordered environments with permanent pathways for the ion transport. This suggests that ionically conducting liquid crystalline polymers (LCPs) which exhibit order and anisotropy may be good candidates for new ionically conducting materials. The ionic conductivity of mixtures of LCP electrolytes and alkali metal salts has been investigated by Wright *et al*. [3–6] and Imrie *et al*. [7–10].

Ionically conducting LCPs may be obtained by introducing a mesogenic group into the polymer backbone of an ionically conducting polymer such as PEO. Such ionically conducting LCPs would have the segmental motions of the ethylene oxides combined with the formation of ionic channels originating in the LC phases [11–13].

Many ionically conducting polymers are known, however the value of ionic conductivity of the polymers themselves is limited. In order to improve this by one or two orders of magnitude, many researchers are seeking new ionically conducting materials instead of PEO. Ionic liquids are intensively investigated because of their properties, such as, non-volatility, incombustibility, chemical stability, and high ionic conductivity [14–19]. In particular, imidazolium salts are well known as one class of ionic liquids resulting from their good physical properties, and application as solvents [20–24]. Furthermore, the ionic conductivity of polymers bearing imidazolium salts has been reported by Ohno *et al*. [25–27].

From the standpoint of low molar mass ionically conducting LC compounds, ammonium salts, pyridinium salts or imidazolium salts with a long alkyl chain readily display smectic phases [28–33]. The salts have the potential to be ionically conducting materials

---

*Corresponding author. Email: nkoide@ch.kagu.sut.ac.jp

Liquid Crystals
ISSN 0267-8292 print/ISSN 1366-5855 online © 2005 Taylor & Francis Ltd
http://www.tandf.co.uk/journals
DOI: 10.1080/02678290412331329152

without mixing with alkali metal salts, although they show poor processability [34–36]. To improve the processability of the salts, we considered the polymerization of monomers containing salts. The resulting polymers would be ionically conducting LCPs that show both ionically conducting and self-assembling properties. The polymers would have ionic pathways resulting from their self-assembling properties.

We have reported already the thermal properties and ionic conductivity of a side chain polymer bearing imidazolium salts [37]. The side chain polymers were prepared by solution radical polymerization. Optical textures characteristic of LC phases were not observed for the side chain polymers, although X-ray diffraction patterns and DSC measurements demonstrated that the side chain polymers exhibited a smectic phase. By contrast, *in situ* photopolymerization using UV irradiation would easily capture the LC structure exhibited by the monomer [38]. An LCP with an imidazolium salt derivative as a terminal group in the side chain was prepared by *in situ* photopolymerization [39].

In this report, we describe the thermal properties and temperature dependence of the ionic conductivity for the side chain polymer prepared by *in situ* photopolymerization of a LC vinylimidazole monomer.

2. Experimental

2.1. *Materials*

A vinylimidazole-based monomer was synthesized according to scheme 1. Intermediates in scheme 1 were prepared according to conventional synthetic methods [40, 41]. Synthetic procedures are described for the vinylimidazole monomer.

2.1.1. 4-Butoxy-4′-(12-bromododecyloxy)biphenyl. ^{1}H NMR (CDCl$_3$) δ ppm: 7.44 (d, 4H, Ar), 6.92 (d, 4H, Ar), 3.98 (m, 4H, OCH$_2$), 3.39 (t, 2H, CH$_2$Br), 1.2–2.0 (m, 24H, CH$_2$), 0.97 (t, 3H, CH$_3$), m.p. 113°C. Elemental analysis: calcd for $C_{28}H_{41}O_2Br$ (489.54), C 68.70, H 8.44; found, C 68.53, H 8.45%.

2.1.2. 1-[12-(4′-Butoxy-4-biphenylyloxy)dodecyl]-3-vinylimidazolium bromide (VIm-12). 4-Butoxy-4′-(12-bromododecyloxy)biphenyl (2.0 g, 4.6 mmol) and a small amount of hydroquinone were dissolved in 1-vinylimidazole (4 ml, 24 mmol). After the reaction mixture was heated at 60°C for 48 h, a viscous liquid was obtained. The viscous liquid was poured into diethyl ether (100 ml), precipitating a white solid. This was dissolved in chloroform and reprecipitated twice with ethyl acetate. The product was purified by washing with diethyl ether; yield 2.2 g, 91%. ^{1}H NMR (CDCl$_3$) δ ppm: 10.95 (s, 1H, imidazolium ring), 7.69 (m, 1H, vinyl group), 7.43 (s, 1H, imidazolium ring), 7.41 (s, 1H, imidazolium ring), 7.38 (d, 4H, Ar), 6.86 (d, 4H, Ar), 5.90, 5.33 (m, 2H, vinyl group), 4.31 (t, 2H, N–CH$_2$), 3.91 (m, 4H, OCH$_2$), 1.19–1.88 (m, 32H, CH$_2$), 0.91 (t, 3H, CH$_3$). IR (KBr) ν cm^{-1}: 3118, 3043 (imidazolium cation), 2919, 2852 (CH$_2$), 1650 (C=C), 1606, 1500 (Ar), 1245, 1272 (Ar–O–CH$_2$), 600 (C=C). Elemental analysis: calcd for $C_{33}H_{47}N_2O_2Br$ (583.66)+H_2O,

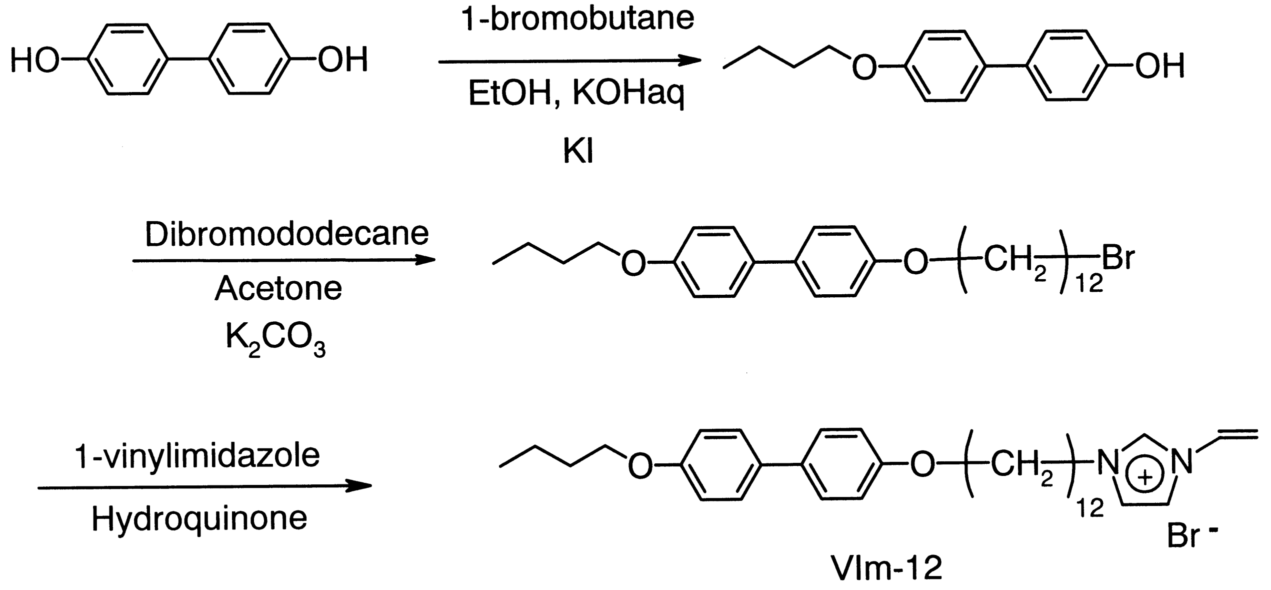

Scheme 1. Synthesis of the vinylimidazole-containing monomer.

C 65.88, H 8.21, N 4.66; found, C 65.71; H 8.10; N 4.72%.

2.2. *Photopolymerization*

A LC vinylimidazole monomer (0.1 g, 0.18 mmol), 2,2-dimethoxy-2-phenylacetophenone (2 wt%) and 4-methoxyphenol (200 ppm) were dissolved in chloroform. The chloroform solution was evaporated to dryness under reduced pressure, and the residue dried *in vacuo*. The mixture was used to fill a cell fabricated from ITO glass plates; the cell gap was 40 µm. The sample in the ITO glass cell was irradiated with UV light at 155°C for 20 min (1.0 mW cm^{-2} at 365 nm). IR (KBr) v cm^{-1}: 3118, 3043 (imidazolium cation), 2925, 2852 (CH_2), 1606, 1500 (Ar), 1245, 1272 (Ar–O–CH_2).

2.8. *Characterization*

^{1}H NMR measurements were carried out with a Jeol JNM-LA 400 spectrometer using $CDCl_3$ as the solvent. Infrared spectra were recorded on a Jeol JIR 7000 spectrometer. Spectra were collected at 4 cm^{-1} resolution. FTIR spectra of the samples were measured using KBr disks. Elemental analyses were carried out using a Perkin Elmer Series II CHNS/O Analyzer 2400.

DSC measurements were conducted with a Mettler DSC822^e equipped with a Hamamatsu Photocure 200 UV-spot light source. Polarizing optical microscopy (POM) measurements were performed on a Nikon polarizing optical microscope, Optiphoto-Pol, equipped with a Mettler FP80 controller and a FP82 hot stage. Thermal properties of the vinylimidazole monomer were investigated by POM and DSC.

X-ray diffraction (XRD) patterns were recorded with a Rigaku RINT2500 with Ni-filtered CuK$_\alpha$ radiation. The sample in a quartz capillary (diameter 1 mm) was held in a temperature-controlled cell (Rigaku LC high temperature controller).

The ionic conductivity of the polymer obtained was measured with an a.c. impedance analyzer (Solartron Co. Impedance/Gain-Phase Analyzer SI 1260) over the frequency range 10–10^6 Hz. Temperature dependence of the ionic conductivity was investigated in the range 30–150°C. The upper temperature for the measurement of ionic conductivity was limited by the thermal stability of the PTFE tape used as a spacer for the cell, which was fabricated by pressing the sample between ITO glass blocking electrodes (1.0 cm^2 electrode surface area, 40 µm spacer thickness). The monomer was dried at 60°C under vacuum for more than 3 days. The fabrication of the cell was carried out in a glove box filled with nitrogen.

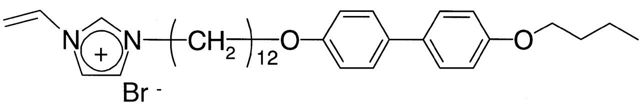

VIm-12

Figure 1. Chemical structure of the LC vinylimidazole monomer.

3. Results and discussion

Figure 1 shows the chemical structure of the LC vinylimidazole monomer (VIm-12). VIm-12 was synthesized by the addition reaction of the calamitic mesogen derivative and 1-vinylimidazole as shown in scheme 1. Cyclic temperature scans in the polarizing optical measurements of VIm-12 were carried out to investigate the occurrence of thermal polymerization of the monomer. The clearing point was not detected after the first heating run; therefore, we discuss the thermal properties of VIm-12 only for the first heating run.

VIm-12 is easily aligned vertically on the glass substrate. The alignment behavior of VIm-12 was detected by the conoscopic POM observation. To obtain homogeneous alignment of VIm-12, we used glass substrates coated with a polyimide film.

The melting of VIm-12 occurred at 132°C and birefringence was observed in the temperature range 132–148°C, indicating that VIm-12 exhibits a mesophase in this temperature range. The optical texture shown in figure 2 (*a*) was observed for VIm-12 in the temperature range 148–169°C, and suggests that the phase is a smectic phase.

The DSC trace of VIm-12 is shown in figure 3. Four major transitions are seen, including a glass transition, as generally observed for polymers. However, a glass transition temperature is seen for VIm-12, even though it is a low molar mass compound. The peaks can be assigned to solid – mesophase, mesophase – mesophase and mesophase – isotropic phase transitions. A focal-conic texture, as shown in figure 2 (*a*), is observed in the temperature range 148–169°C. The results of POM observations indicate that VIm-12 exhibits a smectic phase. A small endothermic peak near 158°C is observed, however no change in the optical texture was detected by POM. We suggest that the appearance of this small peak may arise from the thermal polymerization of VIm-12.

We recorded the FTIR spectrum of VIm-12 after the first heating run to confirm the assignment of the small endothermic peak at 158°C. The peak at 1650 cm^{-1} assigned to the vinyl group in the vinylimidazole moiety slightly decreased in intensity after the first heating. This decrease presumably results from the thermal polymerization of VIm-12, the extent of which, calculated

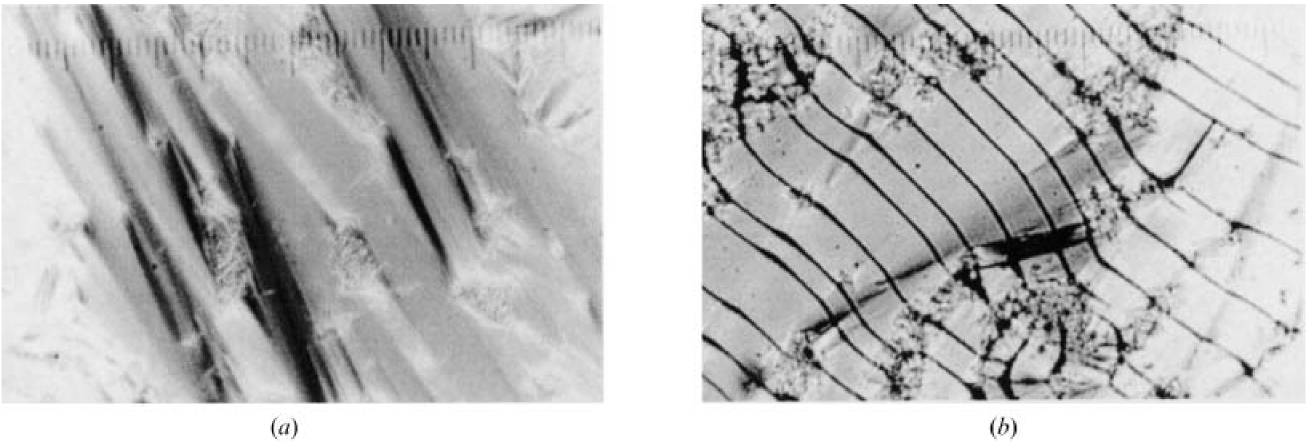

Figure 2. Optical textures of (*a*) LC vinylimidazole monomer and (*b*) the resulting polymer.

from the absorbance ratio (absorbance of peak at 1650 cm^{-1}/absorbance of peak at 1500 cm^{-1}), was about 10% after the first heating run.

XRD measurements were carried out to investigate the phase structure of VIm-12. Figure 4 shows the XRD patterns of VIm-12 at various temperatures. A sharp peak at 4.36° (20.3 Å) and multiple peaks near 20° are observed in the XRD pattern at 25°C. Patterns at 70°C (above the glass transition temperature) and at 140°C are similar to that at 25°C. Two sharp peaks, 2.20° (40.1 Å) and 4.35°, in the small angle region and a broad peak in the wide angle region are detected at 155°C. The *d*-spacing calculated for the diffraction peak at 2.20° is related to the calculated length of the interdigitated bilayer structures formed by VIm-12; while the *d*-spacing based upon the diffraction peak near 4.3–4.4° corresponds to the calculated length of the segments consisting of the imidazolium salt and the alkyl spacer. However, the origin of the peak near 4.3–4.4° is not clear at the present time.

The thermal properties of VIm-12 measured on the first heating scan are summarized in table 1. A typical smectic A phase was observed in the temperature range between 148–169°C; photopolymerization of VIm-12 took place at 155°C.

We investigated the photopolymerization of VIm-12 using UV-DSC observation. Figure 5 shows the isothermal DSC curve for VIm-12 irradiated with UV

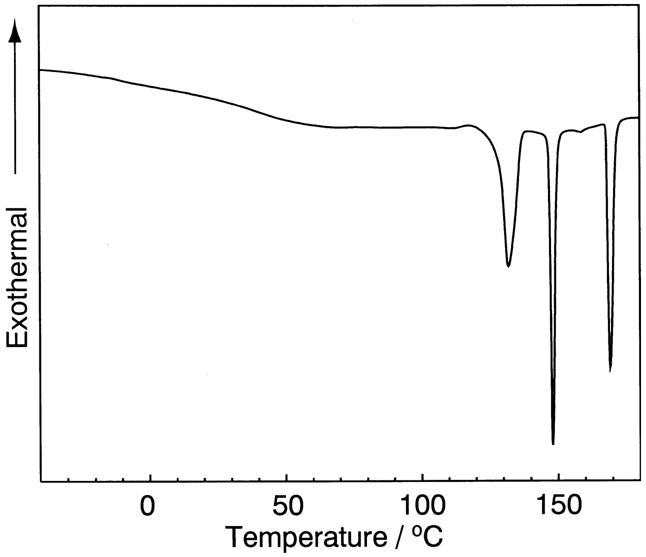

Figure 3. DSC trace of the vinylimidazole monomer on the first heating scan.

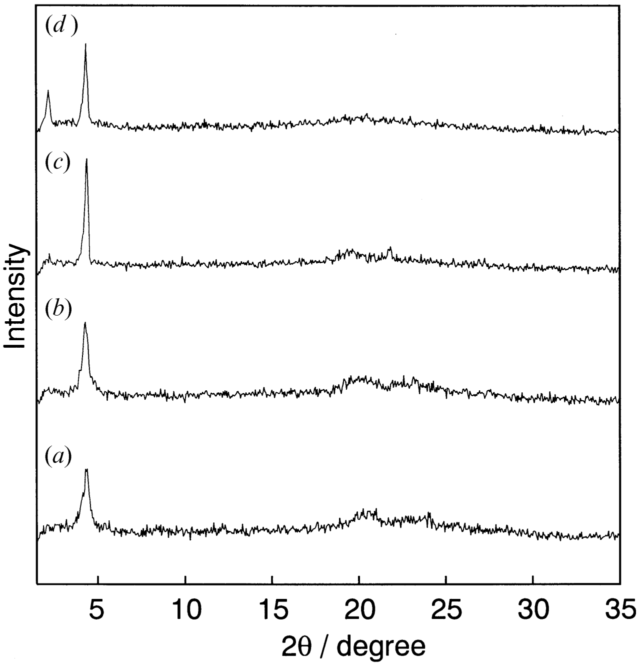

Figure 4. X-ray diffraction patterns of vinylimidazole monomer (*a*) at 25°C, (*b*) at 70°C, (*c*) at 140°C and (*d*) at 155°C.

Table 1. Phase transition temperatures (°C) of the vinylimidazole-containing monomer, VIm-12: g=glassy, S=solid, Sm=smectic phase, I=isotropic phase. Phase transition enthalpies (kJ mol^{-1}) are given in parentheses.

Phase transitions
$\mathrm{g} \xrightarrow{29} \mathrm{S} \xrightarrow{132(11.8)} \mathrm{S} \xrightarrow{148(8.7)} \mathrm{Sm} \xrightarrow{169(7.9)} \mathrm{I}$

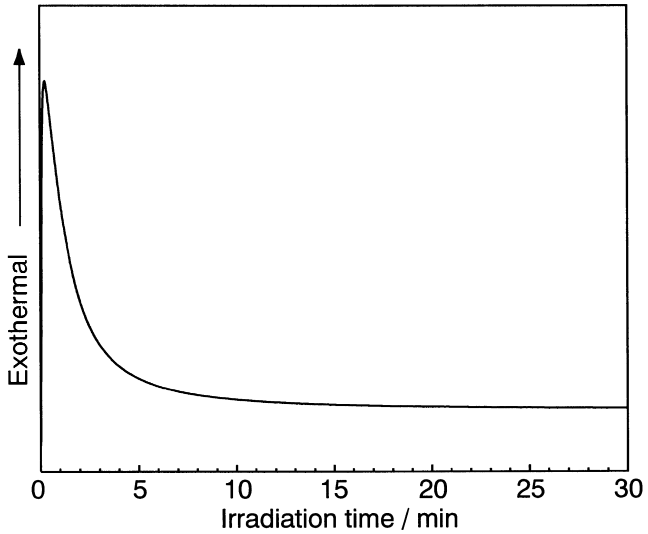

Figure 5. Isothermal UV-DSC trace of the vinylimidazole-containing monomer irradiated with UV light (1.0 mW cm^{-2} at 365 nm) at 155°C.

light (1.0 mW cm^{-2} at 365 nm) at 155°C, and determined the UV irradiation time for photopolymerization. The UV-DSC curve indicates that photopolymerization of VIm-12 is complete in about 17 min; VIm-12 was therefore irradiated with UV light for 20 min.

Figure 6 shows FTIR spectra of VIm-12 and the polymer obtained. The peaks near 1650 and 600 cm^{-1} are not evident in the FTIR spectrum of the polymer. These two peaks are assigned to the vinyl group of the vinylimidazole moiety; their disappearance supports the proposed photopolymerization of VIm-12. The extent of photopolymerization was 64%, calculated from the decrease in their absorbance ratios. The peaks near 3400 cm^{-1} in figure 6 (*a*) and (*b*) are assigned to water vapour absorbed by the KBr disk during the FTIR measurements; at the present time, however, we are unable to determine the water content of KBr salt and the sample (monomer or polymer).

Figure 2 (*b*) shows the optical texture of the polymer prepared by the photopolymerization of VIm-12; it suggests that the phase structure of the polymer is a highly ordered smectic or crystalline phase.

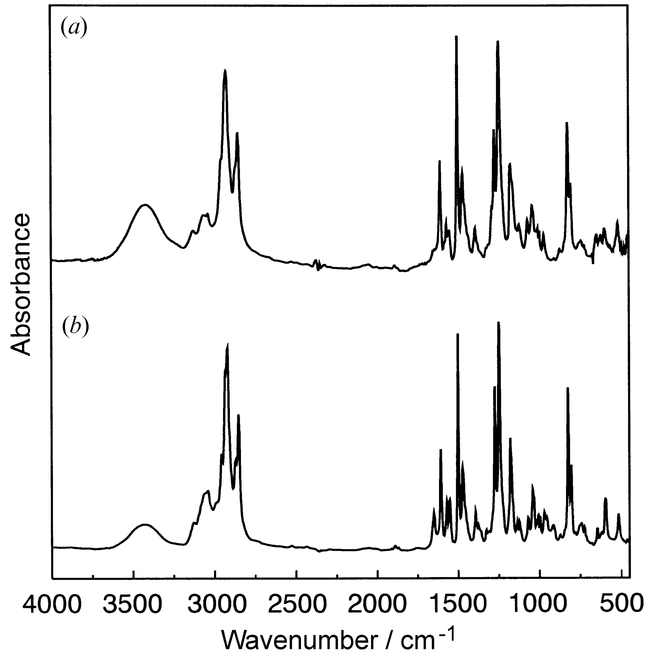

Figure 6. FTIR spectra of (*a*) the polymer prepared by photopolymerization and (*b*) the monomer.

To confirm the phase structure of the polymer, we recorded its XRD pattern in the film state at room temperature, see figure 7. Two sharp peaks in the small angle region and multiple peaks in the wide angle region were detected. The *d*-spacings of the two peaks in the small angle region were 41.1 and 20.8 Å, slightly larger than those of VIm-12. The appearance of multiple peaks in the wide angle region indicates that the

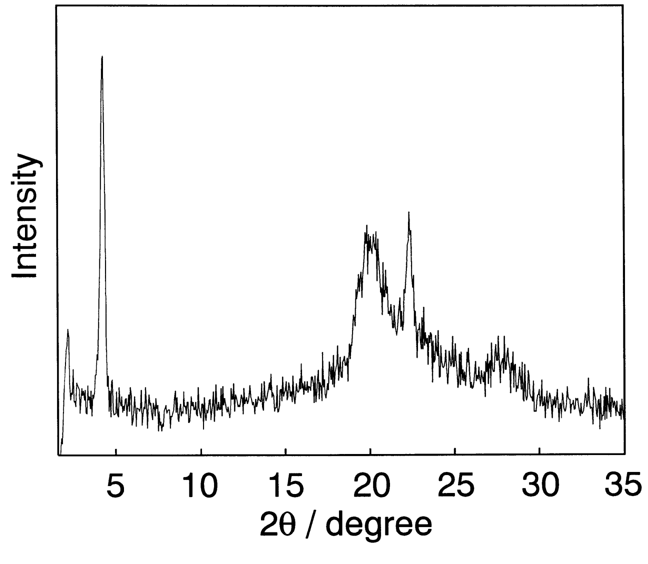

Figure 7. X-ray diffraction pattern of the polymer prepared by photopolymerization of VIm-12.

structure of the polymer could be a highly ordered E phase. The XRD pattern supports the result of POM measurements for the polymer. VIm-12 exhibited a smectic A phase at 155°C, based on observation of the focal-conic texture as shown in figure 2 (*a*) and the XRD pattern in figure 4 (*d*); the XRD pattern of the polymer is indicative of an E phase. Thus the photopolymerization process of VIm-12 leads to a phase transition from smectic A to an E phase. We have already reported that the helical structure of the cholesteric phase of a polymerizable cholesteric monomer can be preserved during photopolymerization [38]. However, the LC phase structure of VIm-12 is not preserved during photopolymerization in the LC state, although details of the photopolymerization process for VIm-12 are not clear at the present time.

The thermal properties of the polymer were investigated by optical microscopy and DSC. The optical texture of the polymer did not change in the temperature range between room temperature and about 200°C. No peaks were detected in the DSC trace of the polymer, therefore the phase structure of the polymer is stable in this temperature range.

We investigated the solubility of the polymer. It was insoluble in water and common organic solvents such as tetrahydrofuran, chloroform, dimethylformamide, ethanol and acetone. This poor solubility suggests that a crosslinked polymer is obtained by photopolymerization. However, a crosslinking reaction cannot occur, because VIm-12 has only one vinyl group in the chemical structure. The solubility of non-crosslinked ionic polymers containing an imidazolium salt is dependent on the counter anion [42]. The interaction between the ionic parts plays an important role in determining the solubility of ionic polymers. Figure 6 shows that the IR spectrum of the polymer is similar to that of the monomer except for the disappearance of the peaks near 1650 and near 600 $\mathrm{cm^{-1}}$ assigned to the vinyl group in the vinylimidazole moiety. These results support the view that a non-crosslinked polymer is obtained by UV irradiation. The poor solubility of the polymer may be attributed to the ionic interactions between the imidazolium salts. The thermal stability of the mesomorphic structure of the polymer may also originate from ionic interactions between the imidazolium salts in the polymer. Thermal decomposition of the polymer occurred before the phase transition to the isotropic melt, imparting a brown colouration above 200°C.

VIm-12 is easily aligned vertically on a glass substrate, as detected by conoscopic observation in POM measurements. By contrast, to obtain the homogeneous alignment of VIm-12, we used glass substrates coated with a polyimide film. Photopolymerization of VIm-12 in either homeotropic or homogeneous alignment was carried out to investigate the anisotropy of the ionic conductivity of the polymer. VIm-12 in an ITO glass cell with no alignment film tends to be aligned perpendicular to the ITO glass substrate (homeotropic alignment). Homeotropic alignment of VIm-12 and the resulting polymer was confirmed by conoscopic POM. On the other hand, to investigate the ionic conductivity of the polymer with homogeneous alignment, a cell was fabricated from ITO glasses coated with a polyimide film. Homogeneous alignment was achieved for the polymer prepared by photopolymerization, as shown in figure 2 (*b*).

We measured the ionic conductivity of the polymer in the temperature range 30–150°C, as calculated from complex impedance plots. Clear semicircular complex impedance plots could not be obtained for the polymer above about 100°C; we therefore restrict the ionic conductivity data to below this temperature. It is not clear why semicircular complex impedance plots could not be obtained at higher temperature.

Figure 8 shows the temperature dependence of the ionic conductivity of two polymer films. The value of the ionic conductivity of both films increases with increasing temperature. The ionic conductivity of the polymer homogeneously aligned is larger than that homeotropically aligned. The difference in the ionic conductivity between the two films arises from the difference in the alignment of the mesogenic groups.

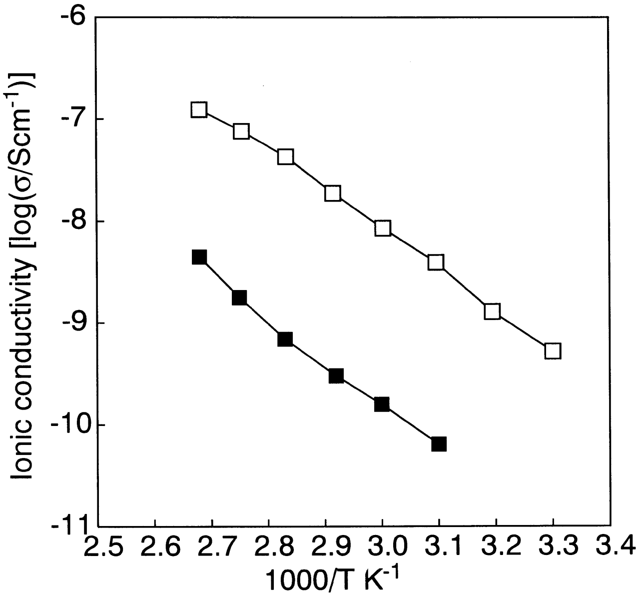

Figure 8. Temperature dependence of ionic conductivity of the polymer with homeotropic alignment (filled squares) and with homogeneous alignment (open squares).

Details of the influence of alignment on the ionic conductivity of the polymer are not clear at the present time, although we note that the ionic conducting behavior of the polyimide alignment film itself was not detected.

The temperature dependence of ionic conductivity is Arrhenius rather than VTF (Vogel–Tamman–Fulcher) dependent, which is often observed for crystalline polymers. The phase structure of the polymer was an E structure, as indicated by figure 7. An E phase is a highly ordered phase and has three-dimensional long range positional and orientational order; therefore, an Arrhenius dependence of the ionic conducting behaviour should be observed for the polymer. A hysteresis of the ionic conducting behavior on the heating and cooling cycles is often observed for ionically conducting crystalline polymers; however, this was not observed here. Presently, we cannot explain why such hysteresis behavior is not observed for our polymer.

4. Conclusion

We have synthesized a liquid crystalline polymer containing an imidazolium salt moiety and a mesogenic group by *in situ* photopolymerization. The monomer shows a smectic A phase, while the polymer displays an E phase in the temperature range between room temperature and about 200°C. The ionic conductivity of the polymer in a homogeneous alignment was larger than that in a homeotropic alignment.

References

[1] J.R. MacCallum, C.A. Vincent (Eds.). *Polymer Electrolyte Review 1 and 2*. Elsevier, London (1987, 1989).

[2] Z. Gadjourova, Y.G. Andreev, D.P. Tunstall, P.G. Bruce. *Nature*, **412**, 520 (2001).

[3] F.G. Dias, S.V. Batty, J.P. Voss, G. Ungar, P.V. Wright. *Solid state Ionics*, **85**, 43 (1996).

[4] F.G. Dias, S.V. Batty, A. Gupta, G. Ungar, J.P. Voss, P.V. Wright. *Electrochim. Acta*, **43**, 1217 (1998).

[5] Y. Zheng, P.V. Wright, G. Ungar. *Electrochim. Acta*, **45**, 1161 (2000).

[6] Y. Zheng, F. Chia, G. Ungar, T.H. Richardson, P.V. Wright. *Electrochim. Acta*, **46**, 1397 (2001).

[7] G.S. McHattie, C.T. Imrie, M.D. Ingram. *Electrochim. Acta*, **43**, 1151 (1998).

[8] C.T. Imrie, M.D. Ingram, G.S. McHattie. *J. phys. Chem. B*, **103**, 4132 (1999).

[9] C.T. Imrie, M.D. Ingram, G.S. McHattie. *Adv. Mater.*, **11**, 832 (1999).

[10] C.T. Imrie, R.T. Inkster, Z. Lu, M.D. Ingram. *Mol. Cryst. liq. Cryst.*, **408**, 33 (2004).

[11] K. Kawamura, T. Kikuchi, N. Koide. *Mol. Cryst. liq. Cryst.*, **318**, 87 (1998).

[12] K. Kawamura, N. Koide. *Koubunshi Ronbunshu*, **56**, 240 (1999).

[13] Y. Akachi, K. Kawamura, N. Koide. *Polym. adv. Tech.*, **12**, 422 (2001).

[14] T. Welton. *Chem. Rev.*, **99**, 2071 (1999).

[15] J.G. Huddleston, H.D. Willauer, R.P. Swatloski, A.E. Visser, R.D. Rogers. *Chem. Commun.*, 1765 (1998).

[16] V.R. Koch, C. Nanjundiah, G.B. Appetecchi, B. Scrosati. *J. Electrochem. Soc.*, **142**, L116 (1995).

[17] N. Papageorgiou, Y. Athanassov, M. Armand, P. Bonhôte, H. Pettersson, A. Azam, M. Grätzel. *J. electrochem. Soc.*, **143**, 3099 (1996).

[18] H. Matsumoto, T. Matsuda, T. Tsuda, R. Hagiwara, Y. Ito, Y. Miyazaki. *Chem. Lett.*, 26 (2001).

[19] M. Doyle, S.K. Choi, G. Proulx. *J. electrochem. Soc.*, **147**, 34 (2000).

[20] P. Bonhôte, A.-P. Dias, N. Papageorgiou, K. Kalyanasundaram, M. Grätzel. *Inorg. Chem.*, **35**, 1168 (1996).

[21] D.R. MacFarlane, J. Huang, M. Forsyth. *Nature*, **402**, 792 (1999).

[22] D.R. MacFarlane, J. Sun, J. Golding, P. Meakin, M. Forsyth. *Electrochim. Acta.*, **45**, 1271 (2000).

[23] R. Hagiwara. *Electrochemistry*, **70**, 130 (2002).

[24] H. Olivier-Bourbigou, L. Magna. *J. mol. Catal. A*, **182–183**, 419 (2002).

[25] M. Hirao, K. Ito-Akita, H. Ohno. *Polym. adv. Technol.*, **11**, 534 (2000).

[26] H. Ohno. *Electrochim. Acta*, **46**, 1407 (2001).

[27] M. Yoshizawa, H. Ohno. *Electrochim. Acta*, **46**, 1723 (2001).

[28] D. Navarro-Rodriguez, Y. Frere, P. Gramain, D. Guillon, A. Skoulios. *Liq. Cryst.*, **9**, 321 (1991).

[29] C.J. Bowlas, D.W. Bruce, K.R. Seddon. *Chem. Commun.*, 1625 (1996).

[30] K.M. Lee, C.K. Lee, I.J.B. Lin. *Chem. Commun.*, 899 (1997).

[31] J.D. Holbrey, K.R. Seddon. *J. chem. Soc., Dalton Trans.*, 2133 (1999).

[32] A.E. Bradley, C. Hardacre, J.D. Holbrey, S. Johnston, S.E.J. McMath, N. Nieuwenhuyzen. *Chem. Mater.*, **14**, 629 (2002).

[33] C.M. Gordon, J.D. Holbrey, A.R. Kennedy, K.R. Seddon. *J. mater. Chem.*, **8**, 2627 (1998).

[34] M. Yoshio, T. Mukai, K. Kanie, M. Yoshizawa, H. Ohno, T. Kato. *Chem. Lett.*, 320 (2002).

[35] M. Yoshio, T. Mukai, K. Kanie, M. Yoshizawa, H. Ohno, T. Kato. *Adv. Mater.*, **14**, 351 (2002).

[36] J.D. Roche, C.M. Gordon, C.T. Imrie, M.D. Ingram, A.R. Kennedy, F.L. Celso, A. Triolo. *Chem. Mater.*, **15**, 3089 (2003).

[37] S. Takada, N. Suzuki, T. Mihara, N. Koide. *Polym. Prepr. Jpn.*, **51**, 737 (2002).

[38] T. Mihara, T. Uedaira, N. Koide. *Liq. Cryst.*, **29**, 855 (2002).

[39] K. Hoshino, M. Yoshio, T. Mukai, K. Kishimoto, H. Ohno, T. Kato. *J. polym. Sci. A, polym. Chem.*, **41**, 3486 (2003).

[40] S. Niemelä, R.S.F. Sundholm, J. Taivainen. *J. macromol. Sci., pure appl. Chem.*, **A29**, 1071 (1992).

[41] L. Cui, V. Sapagovas, G. Lattermann. *Liq. Cryst.*, **29**, 1121 (2002).

[42] R. Marcilla, J.A. Blazquez, J. Rodriguez, J.A. Pomposo, D. Mecerreyes. *J. polym. Sci., A, polym. Chem.*, **42**, 208 (2004).